The Mechanism of Rectification of i_{K1} in Canine Purkinje Myocytes

CARLOS OLIVA, IRA S. COHEN, and PETER PENNEFATHER

From the Department of Physiology and Biophysics, H. S. C., State University of New York at Stony Brook, Stony Brook, New York 11794; and the Faculty of Pharmacy, University of Toronto, Ontario M5S2S2

ABSTRACT We have characterized the inward rectifying background potassium current, i_{K1}, of canine cardiac Purkinje myocytes in terms of its reversal potential, voltage activation curve, and "steady-state" current-voltage relation. The latter parameter was defined from the difference current between holding currents in the presence and absence of 20 mM cesium. Our data suggest that i_{K1} rectification does not arise exclusively from voltage-dependent gating or exclusively from voltage-dependent blockade by internal magnesium ions. The voltage activation curve constructed from tail currents fit to a Boltzmann two-state model predicts less outward current than is actually observed. The magnesium-dependent rectification due to channel blockade is too fast to account for the time-dependent gating of i_{K1} that gives rise to the tail currents. We propose a new model of rectification that assumes that magnesium blockade of the channel occurs simultaneously with voltage-dependent gating. The new model incorporates the kinetic schema elaborated by Matsuda, H. (1988. *J. Physiol.* 397:237–258) to explain the appearance of subconducting states of the i_{K1} channel in the presence of blocking ions. That schema suggested that i_{K1} channels were composed of three parallel pores, each of which could be blocked independently. In our model we considered the consequences of partial blockade of the channel. If the channels are partially blocked at potentials where normally they are mostly gated closed, and if the partially blocked channels cannot close, then blockade will have the paradoxical result of enhancing the current carried by i_{K1}.

INTRODUCTION

The potassium current responsible for inward rectification in the steady-state current-voltage relationship of cardiac myocytes has been called i_{K1} (Isenberg, 1976; DiFrancesco et al., 1984; Shah et al., 1987). The i_{K1} channels activate on hyperpolarization of the membrane, and the single-channel conductance seems to be nearly ohmic (the channel conductance is voltage independent) at potentials negative to the reversal potential of potassium (Sakmann and Trube, 1984; Kurachi, 1985). However, very little or no current passes through the channel in the outward direction (see for instance Sakmann and Trube, 1984; Vandenberg, 1987).

Address reprint requests to Dr. Ira S. Cohen, Department of Physiology and Biophysics, Health Sciences Center, State University of New York at Stony Brook, Stony Brook, NY 11794-8661.

J. GEN. PHYSIOL. © The Rockefeller University Press · 0022-1295/90/08/0299/20 $2.00
Volume 96 August 1990 299–318

It has been proposed that rectification at the single-channel level is due to internal magnesium blockade of the channel when the driving force on the channel is directed outwardly (Matsuda et al., 1987; Vandenberg, 1987). The channel becomes ohmic for outward as well as inward currents when cytoplasmic magnesium concentration is reduced to or below micromolar levels.

Matsuda (1988) found with excised patches that substates of the outwardly conducting channel can be observed. No subconducting states were observed when the channel passed inward current. The subconducting states had one- and two-thirds of the total conductance, and the probabilities of the substates followed binomial distributions which depended on the concentration of magnesium bathing the cytoplasmic face of the i_{K1} channel. From these results, Matsuda hypothesized that the i_{K1} channel was composed of three identical subunits each of which could be independently blocked by one Mg^{2+}. An additional study performed by Matsuda et al. (1989) demonstrated the same distributions of subconducting states with external blockade by Rb^+ or Cs^+ and thus lent further support to the subunit hypothesis.

Blockade of the open channel by magnesium cannot explain all the observed rectifying features of macroscopic i_{K1}. The presence of a hump of outward current at potentials positive to the reversal potential (Shah et al., 1987) implies that the i_{K1} channels are able to pass appreciable outward current with normal $[Mg^{2+}]_i$. Moreover, one can reproduce the general shape of the macroscopic i_{K1} current-voltage relationship from the gating activation curve, ignoring blockade of the channel conductance by Mg^{2+} (Kurachi, 1985; Pennefather and Cohen, 1990). If anything, more outward current is observed than is predicted by simple voltage-dependent gating. In the results presented below we examine the contributions of voltage-dependent gating and voltage-dependent blockade to the macroscopic current-voltage relationship of i_{K1}, taking into account the multibarreled nature of i_{K1} channels. We show that if Mg^{2+} generates partially blocked channels and if those channels with one or more bores blocked cannot close, Mg^{2+} blockade will in fact increase the macroscopic outward current through i_{K1} channels.

METHODS

Preparation of Purkinje strands and the dissociation procedure were as described previously (Cohen et al., 1987). Fibers were also stored overnight in medium (Chang et al., 1989) and dissociated on the second day. No difference in i_{K1} was apparent. The electrophysiologic setup was identical to Cohen et al., 1989, as was the preparation of the electrodes, and the use of an Axopatch amplifier from Axon Instruments Inc., Burlingame, CA. Both series resistance and capacitance compensation were used. The experiments were carried out at 9.6°C.

Solutions

Solution 1. Choline Tyrode external solution contained in millimolar: 5 KCl, 135 choline chloride, 5 HEPES, 0.1 $CdCl_2$, 0.5 $CaCl_2$, 1 $MnCl_2$, pH 7.4. When indicated, choline chloride was replaced by equimolar quantities of KCl or CsCl.

Solution 2. Internal or pipette solution contained in millimolar: 120 KCl, 1 $MgCl_2$, 5 HEPES, 5 EGTA, 5 Na_2ATP, pH 7.2 neutralized with KOH, free Mg^{2+} = 26 μM. In some experiments, the concentration of free Mg^{2+} was increased to 565 μM by reducing the total [ATP] to 1.6 mM and raising the total [$MgCl_2$] to 2.0 mM. The Mg^{2+} activity of the pipette

solutions was calculated using a computer program (CABUFFER) developed by J. Kleinschmidt based on the equations of Goldstein (1979).

Electrophysiological Studies

The data were acquired, digitized, and analyzed with the pCLAMP system (Labmaster/TL-1 interface combination from Axon Instruments Inc.) running in a PC clone. We digitized the data by taking samples every 800 μs. We additionally recorded the data on an FM tape recorder (model 3964a, 3¾ ips, 1,250 Hz bandwidth; Hewlett-Packard Co., Palo Alto, CA).

After breaking the patch and entering the whole-cell patch configuration, we waited ~30 min for some equilibration between the pipette and cell contents. According to Oliva et al. (1988), it takes ~30 min to achieve 90% equilibration when the pipette resistance is 3 MΩ and the diffusion coefficient of the diffusing substance is 10^{-5} cm^2/s.

Protocols and Extraction of Parameters

The voltage-clamp protocols used to determine the activation curve, reversal potential, and steady-state current-voltage relation were generated by the CLAMPEX program of the pCLAMP software package. The holding potential for the protocols was usually the resting potential of the cell which changed with different extracellular potassium concentrations. All experimental values are expressed as mean ± SD.

Activation curve. The activation curve protocol consisted of holding the membrane at different conditioning potentials separated by 5 mV from roughly −50 to +40 mV with respect to the potassium equilibrium potential for 400 ms and then stepping the potential to −30 mV with respect to the potassium equilibrium potential for 400 ms. From the tail currents, we obtained the steady-state ensemble open probability of i_{K1}. We fitted a nonlinear two-state Boltzmann equation to the tail currents vs. conditioning membrane potential data. In doing the fitting we used the first 10 points starting from the most negative potential. Points at potentials positive to the reversal potential of i_{K1} showed scatter, possibly due to overlapping currents at these positive potentials. The equation we fitted to the data was:

$$\delta I = B - \frac{A}{1 + \exp\left[(V - V_d)/s\right]}$$

where δI is the tail current magnitude, V is the conditioning potential, B is the tail current magnitude when V is infinitely positive, A is the difference between B and the tail current when V is infinitely negative, V_d is the midpoint of the activation curve, and s is the slope factor of the activation curve. B, A, V_d, and s are parameters extracted by minimizing the least-squares differences between the observed and predicted tail currents. The ensemble open probability at each test voltage was obtained from the expression $(B - \delta I_V)/A$, where δI_V is the tail current obtained from test voltage V. A, divided by the driving force at the test potential, provided one estimate of the maximal conductance of i_{K1} channels. Conductance values were normalized for cell capacity, which was calculated from the surface area as described by Cohen et al. (1987).

Reversal potential. The reversal potential protocol was just the inverted version of the activation curve protocol. We obtained the reversal potential by interpolating between the two nearest points where the relaxations changed sign.

Steady state current-voltage (I/V) relationship. The steady-state I/V relations of the membrane were measured while the membrane was held at the different potentials of the activation protocol. After 100–150 ms of establishing the potential steps, we averaged 100 ms of the digitized current data. To extract the i_{K1} specific steady-state I/V relationship, we followed a typical procedure (Shah et al., 1987). We obtained the steady-state I/V relationship

in control and in Cs containing external solutions and subtracted the average current values obtained in the two solutions.

We know that

$$I(V) = G(V - V_r)P(V)$$

where I/V is the steady-state channel current at the membrane potential V, G is the maximal ensemble conductance, V_r is the reversal potential for the channels, and $P(V)$ is the steady-state open-channel probability. Therefore, the steady-state I/V curve allowed us to calculate another estimate of the maximal conductance of i_{K1} channels in a cell.

The value of G that minimizes the least-squares differences between the measured and theoretical currents is:

$$G = \frac{\Sigma I_{exp}(V)P(V)(V - V_r)}{\Sigma P^2(V)(V - V_r)^2}$$

where $I_{exp}(V)$ is the current measured when the membrane potential is V. The summations are carried out over the inward currents. In doing this calculation, we make the reasonable assumption that G is not voltage dependent since at potentials appreciably negative to E_K, the channels do not experience blockade (Vandenberg, 1987; Matsuda, 1988), and little inactivation is present in our Na^+-free solutions (see also Biermans et al., 1988).

THEORY

The Model

Our model is basically an extension of the kinetic model that Matsuda (1988) and Matsuda et al. (1989) elaborated to explain the appearance of subconducting states of a single i_{K1} channel distribution. Their data suggested that the channel was composed of three subunits each with equal conductance and that each subunit could be blocked independently by one blocking ion.

The model used to explain that data was:

$$C \underset{\beta}{\overset{\alpha}{\leftrightarrow}} O_3 \underset{\lambda}{\overset{3\mu}{\leftrightarrow}} O_2 \underset{2\lambda}{\overset{2\mu}{\leftrightarrow}} O_1 \underset{3\lambda}{\overset{\mu}{\leftrightarrow}} O_0$$

where C and O_3 are the closed and fully unblocked states, respectively. O_2, O_1, and O_0 represent the states where 1, 2, or 3 subunits are blocked, respectively. α and β are the channel's closed-to-opened and opened-to-closed transition rate constants, respectively. λ and μ are a subunit's blocked-to-opened and opened-to-blocked transition rate constants, respectively. The unblocked and blocked probabilities of subunits are $p = \lambda/(\mu + \lambda)$ and $q = \mu/(\mu + \lambda)$, respectively. The major extension to the model that we made was to incorporate the measured voltage dependence of α and β and to consider the implications of the model for macroscopic currents. We define $P_g = \alpha/(\alpha + \beta)$ and $Q_g = \beta/(\alpha + \beta)$, and estimated P_g from an activation curve protocol.

The set of equations that describes this kinetic schema is:

$$\frac{dC}{dt} = \beta O_3 - \alpha C$$

$$\frac{dO_3}{dt} = \alpha C + \lambda O_2 - O_3(\beta + 3\mu)$$

$$\frac{dO_2}{dt} = (3\mu O_3 + 2\lambda O_1) - O_2(\lambda + 2\mu)$$

$$\frac{dO_1}{dt} = (2\mu O_2 + 3\lambda O_0) - O_1(2\lambda + \mu)$$

$$\frac{dO_0}{dt} = \mu O_1 - 3\lambda O_0$$

$$1 = C + O_3 + O_2 + O_1 + O_0$$

By setting the differential equations equal to zero the steady-state probability distribution of the various states of the channel can be predicted. In the appendix we show that, if the model is correct, the measured steady-state current, I_{exp}, will be determined by gating and blockade as follows:

$$I_{exp} = G(V - V_r)\frac{P_g p}{P_g + Q_g p^3}$$

where G is the conductance when all of the channels are open and unblocked V_r is the reversal potential of the current, and V is the membrane potential.

If the channels were ohmic for potentials negative and positive to their reversal potential, had the activation curve which we denoted by P_g, and did not undergo blockade then the following would hold:

$$I_{ohmic} = G(V - V_r)P_g$$

This implies that:

$$\frac{I_{exp}}{I_{ohmic}} = \frac{p}{P_g + Q_g p^3}$$

Therefore, once one knows the ratio of experimental to ohmic currents and the activation curve, one can estimate p by solving the cubic equation that is generated from the equation above.

Effect of Blockade on the Steady-State Current

Clearly, when $p = 0$ the currents ratio is equal to zero and the channel is always blocked. When $p = 1$, the ratio of experimental to ohmic current is equal to one, the channel is always unblocked behaving like an ohmic-unblockable channel, and any steady-state rectification would be due to the gating of the channel. Intermediate values of p imply there is partial blockade of the channel. Here we show that for certain possible values of P_g and p, the current ratio can be >1. A ratio >1 implies that the ensemble of channels is passing more current than that predicted for an ohmic-unblockable channel ensemble.

For a given value of P_g the value of p that will produce the maximum current ratio >1 can be calculated by setting the derivative of the ratio with respect to p equal to

zero and solving for p_{max} from the resulting equation:

$$\frac{d(I_{exp}/I_{ohm})}{dp} = \frac{P_g - 2Q_g p^3}{(P_g + Q_g p^3)^2}$$

At the maximum:

$$0 = P_g - 2Q_g p_{max}^3; \qquad \text{and } p_{max}^3 = P_g/2Q_g$$

By replacing p_{max} in the equation for the currents ratio, one obtains:

$$\left(\frac{I_{exp}}{I_{ohmic}}\right)_{max} = \frac{2}{3[2(1 - P_g)P_g^2]^{1/3}}$$

For $(I_{exp}/I_{ohmic})_{max}$ to be >1:

$$\frac{[2/3]^3}{2} \simeq 0.1481 > P_g^2(1 - P_g)$$

This inequality holds for all $P_g < 2/3$ implying that for conditions in which $P_g < 2/3$ there exists a value of p where (I_{exp}/I_{ohmic}) is maximally >1. A maximum implies a range of values of p where (I_{exp}/I_{ohmic}) is >1. For a given value of P_g that range can be deduced as follows: If there is a current ratio maximum that is >1 for $0 < p_{max} < 1$ then there should be two different values of p for which the current ratio is smaller than the maximum and equal to 1. One of these values is $p = 1$, and the other value, which we call p_1, can be found by solving the cubic equation of the current ratio.

$$\frac{I_{exp}}{I_{ohmic}} = 1 = \frac{p}{P_g + Q_g p^3}$$

$$0 = p^3 - \frac{p}{Q_g} + \frac{P_g}{Q_g}$$

Since we know one of the roots of this equation (namely, $p = 1$), we only need to solve a quadratic equation to find the other roots. This is clear after factoring the cubic polynomial.

$$p^3 - \frac{p}{Q_g} + \frac{P_g}{Q_g} = (p - 1)[p^2 + p - (P_g/Q_g)]$$

The physically possible root of the quadratic equation (namely $p > 0$) is:

$$p_1 = \frac{-1 + [1 + 4(P_g/Q_g)]^{1/2}}{2} = \left(\frac{1}{4} + P_g/Q_g\right)^{1/2} - \frac{1}{2}$$

Therefore, provided the voltage dependence of gating (P_g) and magnesium blockade (p) are such that there exists a range of potentials where $1 > p > [(1/4 + P_g/Q_g)^{1/2} - 1/2]$ (e.g.; some blockade but not too much) then, in that range of potentials i_{K1} channels will conduct more current in the presence than in the absence of blockade.

This paradox of having the ensemble of channels passing more current at steady state when they are partially blocked as compared with when they are fully unblocked seems counterintuitive. However, this possibility is a logical consequence of the kinetic model. We should remember with this model the channel can go from state to state only in a sequential manner. For the channel to go from any of the blocked states to the closed state, the channel randomly jumps from state to state until it reaches the fully unblocked state from which it could then close. The end result is that the total time the channel spends in conducting states has been elongated due to the "trapping" of the channel in the partially blocked states.

RESULTS

The Whole-Cell Cesium-sensitive I/V Relationships

The steady-state I/V relationship was obtained in two different external potassium concentrations, 12.8 and 5 mM, in control and cesium-containing (20 mM) external solutions. The results in both [K]'s were qualitatively similar so sample figures were chosen from the more physiologic 5 mM [K]. The I/V relationships for one such cell studied in this manner along with raw data from a second cell are illustrated in Fig. 1.

The difference I/V relationship obtained from the data in Fig. 1 *A* (control-cesium) is provided in Fig. 2. The subtracted currents showed little or no time dependence beyond 100 ms suggesting that only time-dependent currents of rapid time course contributed to this difference current. This subtracted I/V is presumed to be the i_{K1} specific I/V relationship (Shah et al., 1987). A thorough account of the experimental evidence that argues for this specificity is relegated to the Discussion.

The Unblockable Channel Model and Our Data

Our aim is to explain the underlying process that is responsible for the features of the i_{K1} I/V relationship illustrated in Fig. 2. As a first approximation, we tested the ability of a simple unblockable channel model to account for the characteristics of the steady-state I/V relationship. The model assumes that the conductance of the open i_{K1} channel is independent of voltage, and therefore the maximal conductance of the macroscopic current is also voltage independent. Only the open-channel probability is assumed to be voltage dependent, and the I/V relationship is obtained by multiplying the maximal conductance, ensemble open probability, and driving force.

Activation curves. We obtained the i_{K1} activation curves at two different external potassium concentrations (12.8 and 5 mM). Fig. 3 illustrates the activation curve obtained from the same cell as Fig. 1 *A*. Samples of tail currents from a second cell are also provided (see inset in the figure). The ensemble open probability increases with hyperpolarization of the cell membrane and the voltage dependence can be accurately fitted using the Boltzmann equation. The solid line is the best fit of the Boltzmann equation to the data.

From the fitting, we extracted the midpoint of activation and slope factor of the activation curve. In 12.8 mM external potassium the average values are -59.7 ± 2.0 mV and 5.9 ± 1.1 mV ($n = 5$), respectively. The average deviation of the midpoint

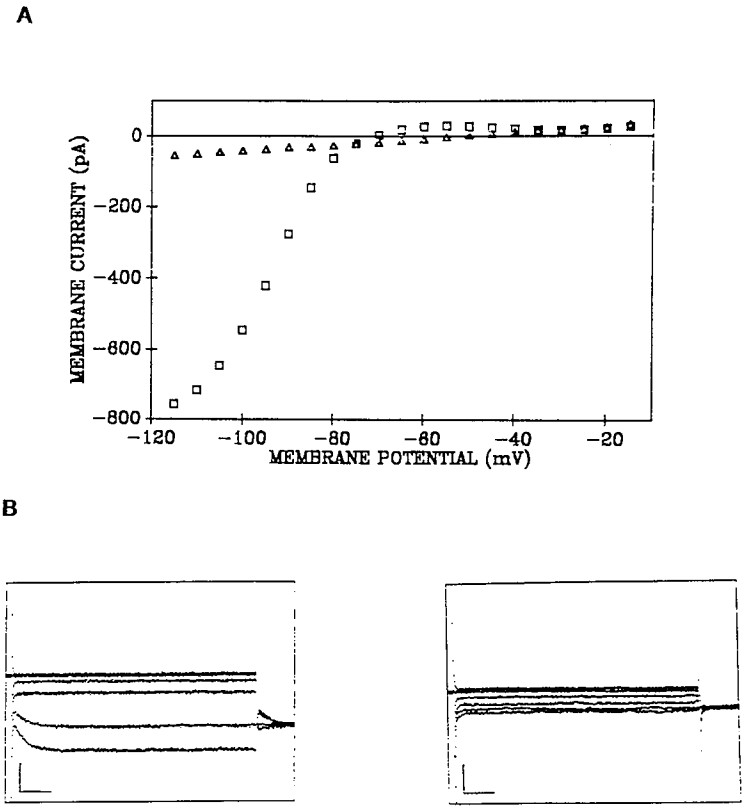

FIGURE 1. (*A*) Steady-state *I/V* relationship in 5 mM K from cell W9131C01. The squares are data obtained in control solution, and the triangles are data obtained when the Tyrode contained 20 mM cesium. (*B*) Raw data from cell W9502C01. The currents were recorded after stepping the membrane potential from a holding potential of −57 to −92, −87, −77, −67, and −52 mV for ~400 ms and then stepping to −87 mV. The panel on the left was recorded in control solution and that on the right in external solution that contained 20 mM cesium. The lengths of the vertical and horizontal scale bars are 200 pA and 50 ms, respectively.

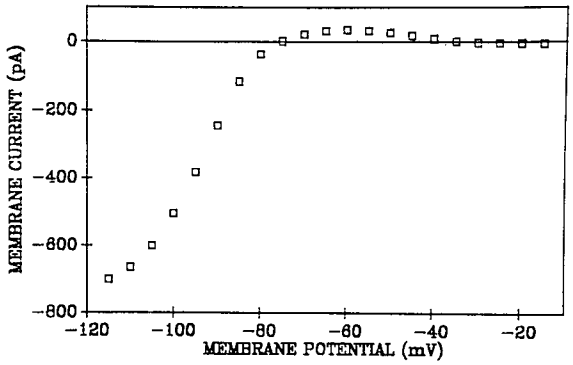

FIGURE 2. Cesium-sensitive *I/V* relationship. The squares are the currents obtained by subtracting the current recorded when there was 20 mM cesium in the extracellular solution from the current recorded in control solution. These cesium-sensitive currents were obtained from the data set shown in Fig. 1 *A*.

of activation from the tail current reversal potential is -7.5 ± 2.2 mV ($n = 5$). Therefore, ~22% of i_{K1} channels are active at the reversal potential. These values agree well with the values obtained previously in similar conditions (Cohen et al., 1989). In 5 mM external potassium, the average values of the midpoint of activation and slope factor are -84.7 ± 6.7 mV and 3.8 ± 0.5 mV ($n = 7$), respectively. The average deviation of the midpoint of activation from the reversal potential is -6.4 ± 1.1 mV and ~16% of i_{K1} channels are active at the reversal potential.

Reversal potential. This parameter was determined from analysis of tail currents as described in Methods. As expected, the reversal potential was less negative when the external potassium concentration was higher. The average reversal potentials were -52.2 ± 3.5 mV ($n = 5$) and -78.3 ± 6.9 mV ($n = 7$) when the external potassium concentrations were 12.8 and 5 mM, respectively. We can compare the reversal potential of i_{K1} obtained from the tail currents with the potential at which the cesium-sensitive current is zero (it is the potential at which the current intercepts

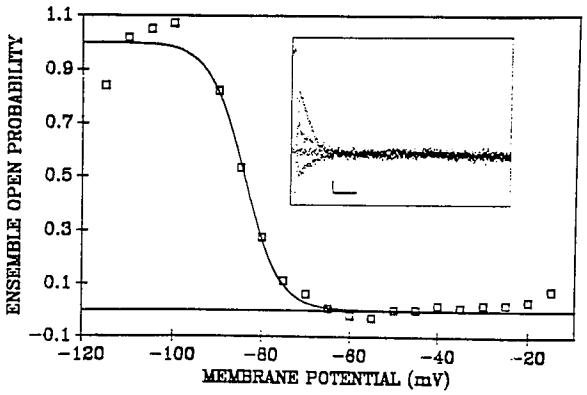

FIGURE 3. Activation curve. The squares are the experimentally obtained steady-state ensemble probabilities and the line through the points is the fit of the Boltzmann equation to the data. The midpoint of activation and slope factor are -82.0 and 3.5 mV, respectively. The graph is from the same cell as Fig. 1 *A*. The inset illustrates sample tail currents from a second data set. The lengths of the vertical and horizontal scale bars are 20 pA and 40 ms. respectively. The holding potential was -57 mV and the test potentials were -97, -87, -82, and -47 mV. The tail currents were recorded at -87 mV. The raw data are from the same cell as in Fig. 1 *B*.

the abscissa). The average values are -50.7 ± 3.8 mV ($n = 5$) and -79.5 ± 8.6 mV ($n = 7$) when the external potassium concentrations are 12.8 and 5 mM, respectively. Thus, the average zero-current potential did not differ by more than a few millivolts from the values obtained from the tail currents.

The measured reversal potentials are close to the expected values for a perfectly selective potassium electrode, -58.4 and -81.3 mV obtained when the external potassium concentrations are 12.8 and 5 mM, respectively, and the cell potassium concentration is 140 mM.

Maximal cesium-sensitive conductance and maximal whole-cell i_{K1} conductance. The final parameter needed to calculate the steady-state current that should flow through channels that behave as predicted by the unblockable channel model is the maximal whole-cell channel ensemble conductance. Therefore, we needed to calculate the specific conductance that results when all of the i_{K1} channels are open. As explained in the Methods, we have two ways of estimating this conductance. We can calculate

the maximal cesium-sensitive conductance or, alternatively, the conductance that derives from one of the parameters obtained by fitting the Boltzmann equation to the tail currents of the activation curve protocol.

We calculated the maximal cesium-sensitive conductance from the steady-state I/V relationship, as explained in the Methods. The average values were 53.4 ± 22.7 $\mu S/\mu F$ ($n = 5$) and 47.0 ± 16.7 $\mu S/\mu F$ ($n = 7$) when the external potassium concentrations were 12.8 and 5 mM, respectively. The average values of the maximal conductances estimated from the tail currents were 43.0 ± 16.0 $\mu S/\mu F$ ($n = 5$) and 39.2 ± 23.3 $\mu S/\mu F$ ($n = 7$) when the external potassium concentrations were 12.8 and 5 mM, respectively.

On average, in 5 mM $[K]_o$ the maximal conductance estimated from the activation curve was 81% of that estimated from the cesium-sensitive I/V ralation. In 12.8 mM $[K]_o$, the estimate of maximal conductance derived from the activation curve was 83% of that estimated from the cesium-sensitive I/V relationship. These differences may reflect a small component of the cesium-sensitive current that does not exhibit

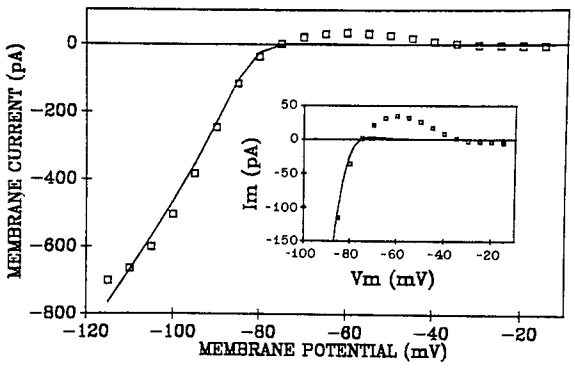

FIGURE 4. Ohmic-unblockable channel model prediction compared with the cesium-sensitive I/V relationship. The lines are the predictions of the ohmic-unblockable channel model and the squares are the experimental cesium-sensitive steady-state currents of Fig. 2. The inset shows that we recorded more outward current than was expected from an ohmic-unblockable channel model.

time-dependent gating. Alternatively, it may reflect problems in estimating the initial amplitude of i_{K1} relaxations induced by voltage jumps.

This reasonably close agreement between the maximal conductances estimated by the two methods implies that the i_{K1} channels exhibiting time-dependent gating are responsible for most of the steady-state cesium-sensitive current flowing at potentials negative to the reversal potential.

The unblockable channel model and steady-state properties. The solid line of Fig. 4 is the predicted steady-state current assuming that the i_{K1} channels are ohmic and unblockable, and the squares are the experimentally measured cesium-sensitive currents already shown in Fig. 2. There is more current in the outward direction than predicted using the unblockable model of the i_{K1} channel.

Fig. 5 is the ratio of currents (I_{exp}/I_{ohmic}). At potentials negative to the reversal potential of the current, this ratio approaches the value of 1, but at potentials positive to the reversal potential the ratio is >1. This finding was present for all but

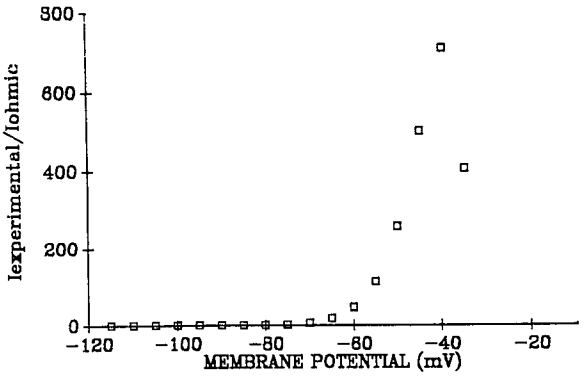

FIGURE 5. Ratios of recorded current to those predicted by the unblockable channel model are plotted for a range of membrane potentials. The values are calculated from the data shown in Fig. 4. Negative to the reversal potential for i_{K1} the ratio is close to 1 as indicated by the excellent fit of theory to the data in Fig. 4. Positive to this reversal the experimental result exceeds the theoretical expectation by a large amount.

one of the cells tested and it implies that the unblockable channel model cannot account for all of the results.

Before examining a more complicated model, we decided to estimate the magnitude of the deviation from a simple Boltzmann two-state model of the voltage dependence of activation. We calculated the activation curve that would allow an unblockable model of the channel to fit the steady-state I/V relationship of i_{K1}.

The plot in Fig. 6 illustrates our results. There is a substantial deviation between the Boltzmann two-state fit to the tail currents and the expected activation curve if the unblockable model was correct. In general this deviation was larger in 5 mM than in 12.8 mM [K], although both deviations were in the same direction. We felt this deviation was large enough to justify the consideration of a more elaborate model to analyze the data, particularly in light of recent single-channel studies demonstrating multiple conducting substates of the i_{K1} channel (Matsuda, 1988; Matsuda et al., 1989).

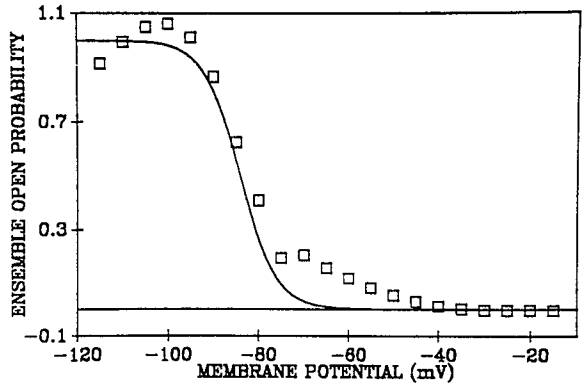

FIGURE 6. Activation curve deviation. The curve is the ensemble open probability calculated by fitting the Boltzmann equation to the tail currents obtained from the activation curve protocol. The squares are the ensemble open probabilities which the ohmic-unblockable channels must have to perfectly reproduce the observed steady-state cesium-sensitive currents. These probabilities were obtained from the cell in Fig. 1 *A*.

A More Elaborate Model

We have found that the excess outward current in the i_{K1} current-voltage relationship can be accounted for if the unblockable model is combined with the Matsuda model (detailed in Theory) of blockade of i_{K1} channels by cytoplasmic Mg^{2+}. Briefly, the Matsuda model assumes that the i_{K1} channel is composed of three subunits each of which can be independently blocked by a Mg^{2+}. Mg^{2+} blocks only outward currents, and the conductance of the open channel is ohmic when the channel is

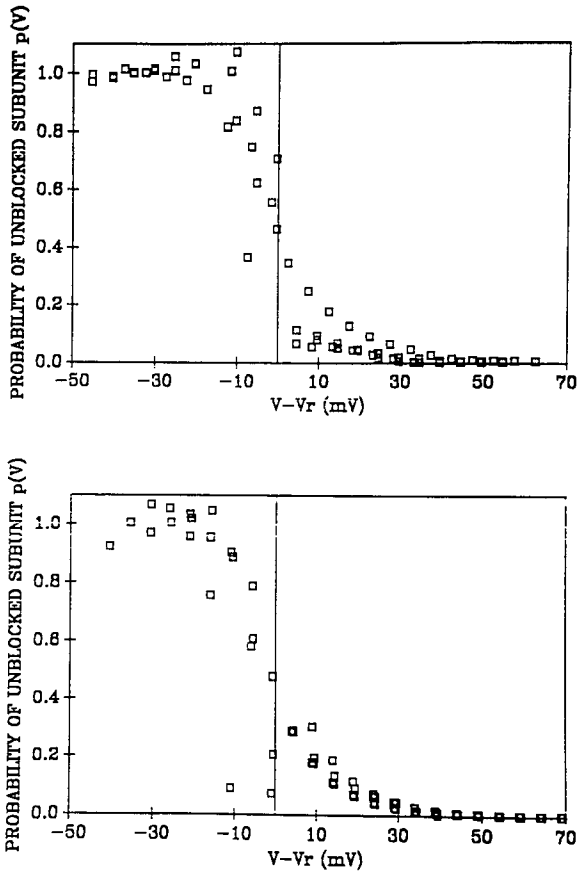

FIGURE 7. Probability of the unblocked subunit. The figure provides summaries of the voltage-dependent probability of the unblocked subunit, p, when the external potassium concentrations are 12.8 (*top*) and 5 mM (*bottom*). The upper panel shows the values calculated for five cells and the lower panel shows the values calculated for seven cells.

passing inward currents. By applying Matsuda's model to our data, we could estimate the voltage dependence of the probability of the unblocked subunit, p (see Theory).

Fig. 7 provides a summary of the values calculated when the external potassium concentration was 12.8 and 5 mM. One can expect two physically possible roots of the cubic equation for p that are consistent with observed currents ratios. We plotted the root of the cubic polynomial that followed a regular pattern of dependence on the membrane potential. The data imply that as the outwardly directed driving force

increases, the probability of the unblocked subunit decreases. The dependence of the absence of blockade on driving force is similar for both $[K^+]$'s.

Our analysis suggests that the probability of the unblocked subunit is a function of $(V - V_r)$ rather than simply V. Also, in accordance with the results obtained previously by other researchers at the single-channel level, we observed that the

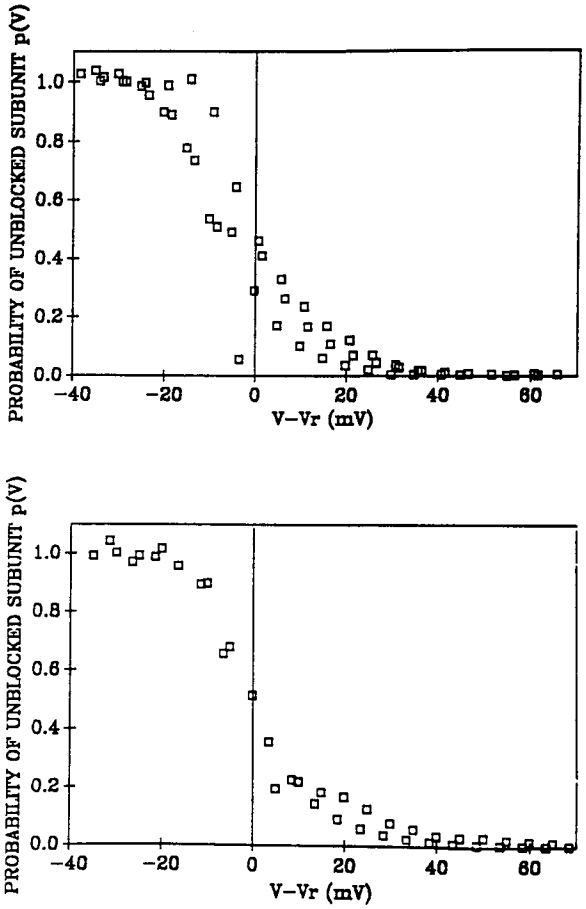

FIGURE 8. Probability of the unblocked subunit, p, when the internal concentration of ATP is low and the internal concentration of Mg^{2+} is high. The pipette solution contains 1.6 mM ATP and 2 mM $MgCl_2$. The upper and lower panels show data obtained when the external potassium concentration was 10 and 5 mM, respectively. The figure shows results for three cells at each of the external potassium concentrations.

probability of the unblocked subunit is very nearly unity at potentials sufficiently negative to the reversal potential of i_{K1} so that single-channel currents could be measured.

High Magnesium and Low ATP

It has been shown that ohmic outward currents through i_{K1} appear when the divalent ion buffering capacity of the pipette solution is high (Vandenberg, 1987; Matsuda et al., 1987). We repeated the whole-cell experiments with a reduced magnesium buffering capacity of the pipette solution. We reduced the ATP concentration of the

pipette solution from 5 to 1.6 mM and increased the $MgCl_2$ concentration from 1 to 2 mM. These changes should have increased the levels of free Mg in the pipette solution from 26 to 565 μM. Results were obtained from three cells in 10 mM K and three cells in 5 mM K. Fig. 8 provides a plot of p vs. membrane potential in the high internal [Mg] at both 5 and 10 mM external [K]. The results are essentially identical to those obtained in Fig. 7 where the pipette [Mg^{2+}] was buffered to low levels by ATP. It is likely, therefore, that in our experiments changing the Mg^{2+} buffering capacity of our pipette solution with ATP had little effect on the intracellular concentration of Mg^{2+}.

DISCUSSION

Separation of Voltage-dependent Gating from Blockade

Our model includes voltage-dependent gating and blockade. In applying the model to the data it is necessary to be able to separate these two processes. We have constructed the activation curve with a two-pulse protocol and have considered the time-dependent tail currents at the test potential as a measure of the voltage-dependent gating process. This assumption is based on previous experimentation by Cohen et al., 1989 in which they examined the properties of i_{K1} at various internal and external [K]'s. They found they could separate a gating process from blockade particularly at reduced internal [K]. Deactivation was examined by using a three-pulse protocol. After an initial hyperpolarization, rectification was rapid on depolarization positive to E_K, and little outward current was observed. However, that rectification was not associated with a rapid recovery of the time-dependent tail current on a second hyperpolarization negative to E_K. Gated closure of the channel took place more slowly (see their Fig. 1). The most reasonable interpretation of this result is that both block on depolarization positive to E_K, and unblock on hyperpolarization negative to E_K are rapid, while the voltage-dependent gating is a slower process. This difference between the rapidity of blockade and the slower kinetics of gating is very prominent at reduced internal [K], but also still discernible at normal internal [K] when the rate of gating becomes more rapid and closer to that of blockade. Matsuda et al. (1987) have also noted that Mg blockade occurs more rapidly than gating. We felt the best measure of the voltage dependence of gating was obtained negative to or just positive to the reversal potential.

Overlap of Other Currents

General considerations. A major premise of this work is that the cesium-sensitive difference current is largely (if not exclusively) i_{K1}. There are several other membrane currents that conceivably could have been altered by Cs^+ and so overlap with and contaminate our measure of i_{K1}. Since Mn^{2+} and Cd^{2+} are present in our solutions, we need not consider i_{Ca} and calcium-mediated currents. Further, many of the potential overlapping currents are time dependent, and thus should have contributed to a time-dependent component of the cesium difference current. No such time dependence was observed. We therefore feel confident in ruling out much overlap from time-dependent current components. Some cardiac currents are only activated at potentials positive to -50 mV (for example i_{Ca}, i_K, and i_{KCa}). We

performed experiments at both 12.8 and 5 mM $[K]_o$ with essentially similar results in all important respects. In 5 mM $[K]_o$ the potentials studied were mostly negative to -50 mV while in 12.8 mM $[K]_o$ they extended above -50 mV.

Cesium block of potassium currents. The selectivity of the Cs^+ blockade of K^+ currents is of relevance to the present study since at least five potassium currents are known to exist in cardiac muscle besides i_{K1} (Pennefather and Cohen, 1990). These include the delayed rectifier, the acetylcholine-dependent potassium current, the ATP-sensitive potassium current, the sodium-dependent potassium current, and the calcium-activated potassium current.

The absence of time dependence in the cesium difference current, and the results in 5 mM $[K^+]_o$ argue against i_K and i_{KCa} contamination. Our pipette [Na] was too low to activate the sodium-dependent K^+ current (Kameyama et al., 1984). Similarly, the pipette ATP concentration exceeded that necessary to block ATP-sensitive potassium channels (Noma and Shibasaki, 1985).

Although low levels of spontaneous activation of i_{KACh} have been reported to exist in cardiac myocytes, these spontaneous channel openings are only a small fraction of the total acetylcholine-induced conductance change and therefore are unlikely to represent a significant contaminant (Soejima and Noma, 1984).

Evaluation of contamination by other currents present in cardiac myocytes. The pacemaker current is time dependent and almost always absent from our Purkinje myocytes in the voltage range -50 to -100 mV (Shah et al., 1987). These characteristics preclude it from being a significant contaminant of our i_{K1} measurements.

Sodium window currents should not be blocked by cesium (Hille, 1975; Sheets et al., 1987). We estimate the change in window current caused by cesium permeability through the sodium channel to be ~1 pA (Oliva, 1989).

The Na/K pump is activated by external cesium as well as potassium (Glitsch et al., 1989). Given our external $[K^+]$ and the reported potency of cesium as an activator of the Na/K pump, we estimate that at 9.6°C cesium addition should increase the pump current by 3 and 1 pA at 5 and 12.8 mM $[K^+]_o$, respectively (Gadsby, 1980; Falk and Cohen, 1984; Glitsch and Pusch, 1984; Cohen et al., 1987; Glitsch et al., 1989).

Reliability of the Estimation of the Probability of the Unblocked Subunit and Comparison with Previous Estimates

Interpreting our data in terms of the new model of rectification of i_{K1}, our experiments indicate that the probability of the unblocked subunit decreases as the membrane is depolarized and that the voltage dependence of blockade shifts according to the shift in the reversal potential of i_{K1}. At potentials sufficiently negative to the reversal potential of i_{K1}, the probability of the unblocked subunit attains the maximum value of 1.

The voltage dependence of the unblocked subunit that we determined was not quantitatively equivalent to the dependence described previously by Matsuda in 1988. Matsuda finds that the probability of the unblocked subunit decreases from 0.48 to 0.30 by changing the membrane potential from +50 to +70 mV (the reversal potential in these experiments was 0 mV). However, at such depolarized

potentials, we find that the probability of the unblocked subunit is much <0.1. That discrepancy could be explained by considering that Matsuda's results were obtained in the presence of only micromolar concentrations of cytoplasmic magnesium and our results were obtained when the cytoplasmic magnesium concentration was at more physiologic levels (see below). The cytoplasmic magnesium concentration in cardiac tissue has been found to be 0.4–3.5 mM (Hess et al., 1982; Blatter and McGuigan, 1986). The probability of the unblocked subunit at a given membrane depolarization decreases as the cytoplasmic magnesium concentration increases (Matsuda et al., 1987; Matsuda, 1988).

Even though in many of our experiments we had 5 mM ATP in the pipette solution, we believe that the Mg^{2+} in the cell was not appreciably chelated. The reasons to believe so were as follows. First, in light of Oliva et al. (1988), a slow equilibration between the pipette and cellular contents is not unexpected. Second, the magnitude and voltage dependence of p were the same whether the pipette solution had a high or low buffer capacity for Mg using ATP as the buffer. Besides, outward currents through i_{K1} have been observed when the cytoplasmic magnesium concentration has been in the micromolar range (Matsuda et al., 1987), and we did not see ohmic outward tail currents attributable to i_{K1} at potentials 40 mV positive to the reversal potential during the course of our experiments.

Physiological Relevance of Mg^{2+} Blockade of Open i_{K1} Channels

Our results support previous suggestions (Kurachi, 1985; Matsuda et al., 1987; Cohen et al., 1989; Pennefather and Cohen, 1990) that voltage-dependent gating of the isomerization between open and closed states of i_{K1} channels accounts for most of their rectification. Negative to E_K, where ~80% of that rectification occurs, the change in steady-state conductance due to i_{K1} is accurately described by a Boltzmann two-state model that reflects the gating process (see Fig. 6). Positive to E_K there is more current than expected from such a simple model.

We have shown that in theory blockade of i_{K1} channels by intracellular Mg^{2+} could account for the enhancement of outward current through i_{K1} channels if partial blockade of the multibarreled i_{K1} channel prevents the unblocked bores of the channel from closing (see Matsuda, 1988). Therefore, instead of inducing inward rectification, Mg^{2+} blockade of i_{K1} channels could oppose inward rectification and could insure that there is appreciable i_{K1} conductance tens of millivolts postive to E_K despite strong voltage dependence of gating around E_K.

We have used the observed extra outward i_{K1} current to predict the relation between V and p, the probability that a bore of the triple barreled i_{K1} channel is not blocked by Mg^{2+}. That relationship is consistent with the lack of blockade by Mg^{2+} of inward currents since the relation approaches 1, 10 mV negative to V_K with either 5 or 12.8 mM $[K]_o$. The dependence of the Mg^{2+} blockade on V_K and the rather steep voltage dependence of that blockade (see Fig. 7) suggests that external K^+ is one of the determinants of the voltage dependence of p.

The system is finely poised for enhancing outward current through i_{K1} channels. As discussed in the Theory section, the voltage dependence of Mg^{2+} blockade and of activation of the i_{K1} channel must be such that p is not too big nor too small for any

given value of P_g. The fact that both parameters are a function of $(V - V_K)$ will insure that the balance is maintained in the face of fluctuations of extracellular K.

APPENDIX

The kinetic schema that describes the model elaborated by Matsuda in 1988 is described in the subsection The Model of the Theory section, as are the differential equations that describe the kinetic model. What follows are the mathematical implications of setting the differential equations equal to zero. We set them equal to zero to analyze the steady-state implications of the kinetic schema:

$$0 = O_3\beta - C\alpha \tag{1}$$

$$0 = O_2\lambda - 3O_3\mu + C\alpha - O_3\beta \tag{2}$$

$$0 = 3O_3\mu + 2O_1\lambda - O_2(\lambda + 2\mu) \tag{3}$$

$$0 = 2O_2\mu + 3O_0\lambda - O_1(2\lambda + \mu) \tag{4}$$

$$0 = O_1\mu - 3O_0\lambda \tag{5}$$

From Eq. 1 one obtains:

$$C = O_3\frac{\beta}{\alpha} \tag{6}$$

The result of replacing C in Eq. 2 and rearranging is:

$$O_2 = O_3\frac{3\mu}{\lambda} \tag{7}$$

By replacing O_2 from Eq. 7 into Eq. 3 and rearranging, one obtains:

$$O_1 = O_3\frac{3\mu^2}{\lambda^2} \tag{8}$$

By replacing O_1 from Eq. 8 into Eq. 5 and rearranging, one obtains:

$$O_0 = O_3\frac{\mu^3}{\lambda^3} \tag{9}$$

We should remember that:

$$C + O_3 + O_2 + O_1 + O_0 = 1 \tag{10}$$

By replacing into Eq. 10 the expressions for the corresponding states (C, O_2, O_1, O_0) shown in Eqs. 6–9 and rearranging, one obtains:

$$O_3\left(\frac{\beta}{\alpha} + \frac{\lambda^3 + 3\mu\lambda^2 + 3\mu^2\lambda + \mu^3}{\lambda^3}\right) = 1 \tag{11}$$

We should remember that $P_g = \alpha/(\alpha + \beta)$ and $Q_g = \beta/(\alpha + \beta)$. Therefore, $Q_g/P_g = \beta/\alpha$. By replacing this ratio into Eq. 11 and rearranging, one obtains:

$$O_3\left[\frac{Q_g}{P_g} + \frac{(\lambda + \mu)^3}{\lambda^3}\right] = 1 \tag{12}$$

We should remember that $p = \lambda/(\lambda + \mu)$. Therefore, $p^3 = [\lambda/(\lambda + \mu)]^3$. By replacing p^3 into the above equation and rearranging, one obtains:

$$O_3 = \frac{P_g p^3}{P_g + Q_g p^3} \tag{13}$$

By replacing the expression for O_3 from Eq. 13 into Eq. 6 and rearranging, one obtains:

$$C = \frac{Q_g p^3}{P_g + Q_g p^3} \tag{14}$$

By replacing the expression for O_3 from Eq. 13 into Eqs. 7–9 and rearranging, we can find the steady-state fraction of channels in states O_2, O_1, and O_0, respectively. The final expressions follow.

$$O_2 = \frac{3\mu}{\lambda} \frac{P_g p^3}{(P_g + Q_g p^3)} \tag{15}$$

$$O_1 = \frac{3\mu^2}{\lambda^2} \frac{P_g p^3}{(P_g + Q_g p^3)} \tag{16}$$

$$O_0 = \frac{\mu^3}{\lambda^3} \frac{P_g p^3}{(P_g + Q_g p^3)} \tag{17}$$

If there are N channels in the cell, the steady-state number of channels in each of the channels states is NC, NO_3, NO_2, NO_1, and NO_0. The channel states that conduct current are O_3, O_2, and O_1. States O_2 and O_1 have two thirds and one third of the conductance of state O_3. Therefore, if we denote by g_0 the conductance of state O_3, then the conductances of states O_2 and O_1 would be $g_0(2/3)$ and $g_0(1/3)$, respectively. To calculate the steady-state current flowing through the channels, one has to multiply the steady-state number of channels in each of the channel states by the conductance of the respective states, multiply these products by the driving force, and finally add all these products. To simplify the equations, one can neglect the channels in states C and O_0 because the conductances of these states are nil. The steady-state ensemble current is:

$$I = g_0 N(V - V_r) \frac{P_g p^3}{P_g + Q_g p^3} \left[1 + \frac{2(3\mu)}{3\lambda} + \frac{3\mu^2}{3\lambda^2}\right] \tag{18}$$

where $(V - V_r)$ is the driving force at the voltage V if the reversal potential is V_r. By rearranging, one obtains:

$$I = g_0 N(V - V_r) \frac{P_g p^3}{P_g + Q_g p^3} \frac{(\lambda + \mu)^2}{\lambda^2} \tag{19}$$

We should remember that $p = \lambda/(\lambda + \mu)$. Therefore, by replacing p into the above equation, one obtains:

$$I = g_0 N(V - V_r) \frac{P_g p}{P_g + Q_g p^3} \tag{20}$$

This is the equation we showed in the Theory section. It only remains to define $g_0 N = G$, the maximal ensemble conductance.

Note added in proof. Since our original submission, a report has appeared which employs a similar model to that presented above (Ishihara et al. 1989. *Journal of Physiology.* 419:297–320) to explain i_{K_1} rectification in guinea pig ventricular myocytes based on quite different experimental protocols.

We would like to thank Dr. D. DiFrancesco for helpful discussion. We would also like to thank Ms. Judy Samarel and Ms. Joan Zuckerman for technical assistance.

This work was supported by HL-20558 and HL-28958 and the Medical Research Council of Canada. P. Pennefather is a career scientist of the Ontario Ministry of Health.

Original version received 16 October 1989 and accepted version received 10 March 1990.

REFERENCES

Biermans, G., J. Vereecke, and E. Carmeliet. 1988. The mechanism of the inactivation of the inward rectifying K current during hyperpolarizing steps in guinea-pig ventricular myocytes. *Pflügers Archiv.* 410:604–613.

Blatter, L. A., and J. A. S. McGuigan. 1986. Free intracellular magnesium concentration in ferret ventricular muscle measured with ion selective micro-electrodes. *Quarterly Journal of Experimental Physiology.* 71:467–473.

Chang, F., J. Gao, C. Tromba, I. Cohen, and D. DiFrancesco. 1990. Acetylcholine reverses the effects of β agonists on i_f in canine cardiac Purkinje fibers but has no direct action: a difference between primary and secondary pacemakers. *Circulation Research.* 66:633-636.

Cohen, I. S., N. B. Datyner, G. A. Gintant, N, K. Mulrine, and P. Pennefather. 1987. Properties of an electrogenic sodium-potassium pump in isolated canine Purkinje myocytes. *Journal of Physiology.* 383:251–267.

Cohen, I. S., D. DiFrancesco, N. K. Mulrine, and P. Pennefather. 1989. Internal and external K^+ help gate the inward rectifier. *Biophysical Journal.* 55:197–202.

DiFrancesco, D., A. Ferroni, and S. Visentin. 1984. Barium-induced blockade of the inward rectifier in calf Purkinje fibers. *Pflügers Archiv.* 402:446–453.

Falk, R. T., and I. S. Cohen. 1984. Membrane current following activity in canine cardiac Purkinje fibers. *Journal of General Physiology.* 83:771–799.

Gadsby, D. C. 1980. Activation of electrogenic Na^+/K^+ exchange by extracellular K^+ in canine cardiac Purkinje fibers. *Proceedings of the National Academy of Sciences.* 77:4035–4039.

Glitsch, H. G., T. Krahn, and F. Verdonck. 1989. Activation of the Na pump current by external K and Cs ions in cardioballs from sheep Purkinje fibres. *Pflügers Archiv.* 414:99–101.

Glitsch, H. G., and H. Pusch. 1984. On the temperature dependence of the Na pump in sheep Purkinje fibers. *Pflügers Archiv.* 402:109–115.

Goldstein, D. A. 1979. Calculation of the concentrations of free cations and cation-ligand complexes in solutions containing multiple divalent cations and legends. *Biophysical Journal.* 26:235–242.

Hess, P., P. Metzger, and R. Weingart. 1982. Free magnesium in sheep, ferret and frog striated muscle at rest measured with ion-selective micro-electrodes. *Journal of Physiology.* 333:173–188.

Hille, B. 1975. Ionic selectivity, saturation, and block in sodium channels. A four-barrier model. *Journal of General Physiology.* 66:535–560.

Isenberg, G. 1976. Cardiac Purkinje fibers: cesium as a tool to block inward rectifying potassium currents. *Pflügers Archiv.* 365:99–106.

Kameyama, M., M. Kakei, R. Sato, T. Shibasaki, H. Matsuda, and H. Irisawa. 1984. Intracellular Na^+ activates a K^+ channel in mammalian cardiac cells. *Nature.* 309:354–356.

Kurachi, Y. 1985. Voltage-dependent activation of the inward-rectifier potassium channel in the ventricular cell membrane of guinea-pig heart. *Journal of Physiology.* 366:365–385.

Matsuda, H. 1988. Open-state substructure of inwardly rectifying potassium channels revealed by magnesium block in guinea-pig heart cells. *Journal of Physiology.* 397:237–258.

Matsuda, H., H. Matsuura, and A. Noma. 1989. Triple-barrel structure of inwardly rectifying K^+ channels revealed by Cs^+ and Rb^+ block in guinea-pig heart cells. *Journal of Physiology.* 413:139–157.

Matsuda, H., A. Saigusa, and H. Irisawa. 1987. Ohmic conductance through the inwardly rectifying K channel and blocking by internal Mg^{+2}. *Nature.* 325:156–159.

Noma, A., and T. Shibasaki. 1985. Membrane current through adenosine-triphosphate-regulated potassium channels in guinea-pig ventricular cells. *Journal of Physiology.* 363:463–480.

Oliva, C. 1989. Diffusion in whole cell patch clamp configuration and mechanism of rectification of i_{K1}. PhD dissertation, SUNY at Stony Brook.

Oliva, C., I. S. Cohen, and R. T. Mathias. 1988. Calculation of time constants for intracellular diffusion in whole cell patch clamp configuration. *Biophysical Journal.* 54:791–799.

Pennefather, P., and I. S. Cohen. 1990. Molecular mechanisms of cardiac potassium channel regulation. *In* Cardiac Eelctrophysiology and Arrythmias from Cell to Bedside. D. P. Zipes and J. Jalife, editors. W. B. Saunders and Co., NY.

Sakmann, B., and G. Trube. 1984. Conductance properties of single inwardly rectifying potassium channels in ventricular cells from guinea-pig heart. *Journal of Physiology.* 347:641–657.

Shah, A. K., I. S. Cohen, and N. Datyner. 1987. Background K^+ current in isolated canine Purkinje myocytes. *Biophysical Journal.* 52:519–525.

Sheets, M. F., B. E. Scanley, D. A. Hanck, J. C. Makielski, and H. A. Fozzard. 1987. Open sodium channel properties of single canine cardiac Purkinje cells. *Biophysical Journal.* 52:13–22.

Soejima, M., and A. Noma. 1984. Mode of regulation of the ACh-sensitive K-channel by the muscarinic receptor in rabbit atrial cells. *Pflügers Archiv.* 400:424–431.

Vandenberg, C. A. 1987. Inward rectification of a potassium channel in cardiac ventricular cells depends on internal magnesium ions. *Proceedings of the National Academy of Sciences.* 84:2560–2564.